

Mechanisms for production of hypernuclei beyond the neutron and proton drip lines

N. Buyukcizmeci,^{1,2} A.S. Botvina,^{2,3,4} J. Pochodzalla,^{4,5} M. Bleicher²

¹*Department of Physics, Selcuk University, 42079 Kampus, Konya, Turkey*

²*Frankfurt Institute for Advanced Studies,*

J. W. Goethe University, D-60438 Frankfurt am Main, Germany

³*Institute for Nuclear Research, Russian Academy of Sciences, 117312 Moscow, Russia*

⁴*Helmholtz-Institut Mainz, J. Gutenberg-Universität, D-55099 Mainz, Germany and*

⁵*Institut für Kernphysik and PRISMA Cluster of Excellence,*

J. Gutenberg-Universität, D-55099 Mainz, Germany

(Dated: October 15, 2018)

Abstract

We analyze hypernuclei coming from fragmentation and multifragmentation of spectator residues obtained in relativistic ion collisions. These hypernuclei have a broad distribution in masses and isospin. They reach beyond the neutron and proton drip lines, and they are expected to be stable with respect to neutron and proton emission. This gives us the opportunity to investigate the properties of exotic hypernuclei, as well as the properties of normal nuclei beyond the drip lines, which can be produced after weak decay of such hypernuclei.

PACS numbers: 21.80.+a, 25.70.Mn, 25.70.Pq, 24.60.-k

I. INTRODUCTION

In high-energy nuclear reactions strange hadrons (baryons and mesons) are produced abundantly, and they are strongly involved in the reaction process. When strange baryons (hyperons) are captured by nuclei, hypernuclei are formed, which can live long enough in comparison with nuclear reaction times. The detailed study of hypernuclei is essential to overcome the very limited experimental possibilities of exploring hyperon-nucleon (YN) and hyperon-hyperon (YY) interactions in elementary scattering experiments ($Y = \Lambda, \Sigma, \Xi, \Omega$). Double- and multi-strange nuclei are especially interesting, because they can provide information about the hyperon-hyperon interaction and strange matter properties. Studying hypernuclei helps us to understand the structure of conventional nuclei too [1], and to extend the nuclear chart into the strangeness sector [2, 3]. Strangeness is an important conception for the construction of theoretical models of strong interactions [4]. It is also important that hyperons should be abundantly produced in nuclear matter at high densities, which are realized in the core of neutron stars [5]. To describe these astrophysical conditions realistically it is necessary to study all aspects of hyperon interactions in the laboratory and select theoretical models which pass careful comparison with experimental data.

Traditionally, information about hypernuclei is obtained from spectroscopy [1]. The theoretical studies are mainly concentrated on calculating the structure of nearly cold hypernuclei with a baryon density around the nuclear saturation density, $\rho_0 \approx 0.15 \text{ fm}^{-3}$. However, a quite limited set of reactions was generally used for producing hypernuclei: Reactions with the production of few particles, including kaons, are quite effective for triggering single hypernuclei, and by using kaon beams one can produce double hypernuclei. The goal of this paper is to demonstrate that one can essentially extend the frame of hypernuclear studies and produce exotic hypernuclei if new many-body reactions are involved.

One should remember that hyperons were discovered in the 1950s in reactions of nuclear multifragmentation induced by cosmic rays [6]. During the last 20 years of research great progress has been made in the investigation of multifragmentation reactions, mainly associated with heavy-ion collisions (see, e.g., [7–10] and references therein). This gives us the opportunity to apply a well-known theoretical method adopted for description of these reactions for production of hypernuclei too [11, 12]. On the other hand, it was noticed long ago that the absorption of hyperons in spectator regions of peripheral relativistic ion collisions

is a promising way to produce hypernuclei [13–16]. Also, central collisions of relativistic heavy ions can lead to the production of light hypernuclei [17]. Corresponding experimental evidence has been reported [18, 19]. Recent sophisticated experiments have confirmed observations of hypernuclei in such reactions, in both peripheral [20] and central collisions [21].

Here we pay special attention to the formation of hypernuclei in the spectator region of peripheral relativistic ion collisions. Current research concerns mainly light hypernuclei produced in reactions with light projectiles [20, 22]. However, there is a promising opportunity to study the production of large and exotic hypernuclei coming from reactions with large projectiles and targets [16, 23]. In particular, multifragmentation decay of excited hyperspectator matter is a perspective mechanism [11, 12]. Below we investigate how exotic (neutron-rich and proton-rich) hypernuclei can be obtained in future experiments.

II. FORMATION AND DISINTEGRATION OF HYPERON-RICH SPECTATOR MATTER

A detailed picture of peripheral relativistic heavy-ion collisions has been established in many experimental and theoretical studies. Nucleons from overlapping parts of the projectile and target (participant zone) interact strongly with themselves and with other hadrons produced in primary and secondary collisions. Nucleons from nonoverlapping parts do not interact intensively, and they form residual nuclear systems, which we call spectators. In all transport models the production of hyperons is associated with nucleon-nucleon collisions, e.g., $p+n \rightarrow n+\Lambda+K^+$, or collisions of secondary mesons with nucleons, e.g., $\pi^++n \rightarrow \Lambda+K^+$. Strange particles can be produced in the participant zone, however, particles can rescatter and undergo secondary interactions. As a result the hyperons produced populate the whole momentum space around the colliding nuclei, including the vicinity of nuclear spectators. Such hyperons can be absorbed by the spectators if their kinetic energy (in the rest frame of the spectator) is lower than the potential generated by neighboring spectator nucleons. The process of formation of spectator hypermatter was investigated in Ref. [16] within transport approaches: the Dubna cascade model (DCM) and ultra-relativistic quantum molecular dynamics (UrQMD) model. It was concluded that already at a beam energy of 2 A GeV single and double hyperspectators can be noticeably produced, while at an energy of

a few tens of giga-electron volts per nucleon the formation of multistrange hyperspectators becomes feasible.

In the following these excited spectators disintegrate in normal nuclei and nuclei containing hyperons. As our calculations and analyses of experimental data obtained in similar heavy-ion reactions [7–10] show, the residual spectator nuclei have rather high excitation energies, and consequently, they should undergo multifragmentation with a characteristic time of about 100 fm/c. Generalization of the statistical multifragmentation model (SMM) [7] into the strangeness sector by including Λ hyperons has been done in Ref. [11]. Here we summarize it.

The model assumes that a hot nuclear spectator with total mass (baryon) number A_0 , charge Z_0 , number of Λ hyperons H_0 , and temperature T expands to a low density freeze-out volume, where the system is in chemical equilibrium. The statistical ensemble includes all breakup channels composed of nucleons and excited fragments with mass number A , charge Z , and number of Λ 's H . The primary fragments are formed in the freeze-out volume V . We use the excluded volume approximation $V = V_0 + V_f$, where $V_0 = A_0/\rho_0$ ($\rho_0 \approx 0.15 \text{ fm}^{-3}$ is the normal nuclear density), and parametrize the free volume $V_f = \kappa V_0$, with $\kappa \approx 2$ [8–10].

Nuclear clusters in the freeze-out volume are described as follows: Light fragments with mass number $A < 4$ are treated as elementary particles with corresponding spin and translational degrees of freedom ("nuclear gas"). Their binding energies were taken from experimental data [1, 7, 24]. Fragments with $A = 4$ are also treated as gas particles with table masses, however, some excitation energy is allowed $E_x = AT^2/\varepsilon_0$ ($\varepsilon_0 \approx 16 \text{ MeV}$ is the inverse volume level density parameter [7]), which reflects the presence of excited states in ${}^4\text{He}$, ${}^4_{\Lambda}\text{H}$, and ${}^4_{\Lambda}\text{He}$ nuclei. Fragments with $A > 4$ are treated as heated liquid drops. In this way one can study the nuclear liquid-gas coexistence of hypermatter in the freeze-out volume. The internal free energies of these fragments are parametrized as the sum of the bulk (F_A^B), the surface (F_A^S), the symmetry (F_{AZH}^{sym}), the Coulomb (F_{AZ}^C), and the hyper (F_{AH}^{hyp}) energies:

$$F_{AZH}(T, V) = F_A^B + F_A^S + F_{AZH}^{\text{sym}} + F_{AZ}^C + F_{AH}^{\text{hyp}} . \quad (1)$$

The first three terms are written in the standard liquid-drop form [7]:

$$F_A^B(T) = \left(-w_0 - \frac{T^2}{\varepsilon_0} \right) A, \quad (2)$$

$$F_A^S(T) = \beta_0 \left(\frac{T_c^2 - T^2}{T_c^2 + T^2} \right)^{5/4} A^{2/3}, \quad (3)$$

$$F_{AZH}^{\text{sym}} = \gamma \frac{(A - H - 2Z)^2}{A - H}. \quad (4)$$

The model parameters $w_0 = 16$ MeV, $\beta_0 = 18$ MeV, $T_c = 18$ MeV and $\gamma = 25$ MeV were extracted from nuclear phenomenology and provide a good description of multifragmentation data [7–10]. The Coulomb interaction of the fragments is described within the Wigner-Seitz approximation, and F_{AZ}^C is taken as in Ref. [7].

The new term is the free hyperenergy F_{AH}^{hyp} . We assume that it does not change with temperature, i.e., it is determined solely by the binding energy of the hyperfragments. We have suggested the liquid-drop hyperenergy term [11]

$$F_{AH}^{\text{hyp}} = (H/A) \cdot (-10.68A + 21.27A^{2/3}). \quad (5)$$

In this formula the binding energy is proportional to the fraction of hyperons in the system (H/A). The second part represents the volume contribution reduced by the surface term and thus resembles a liquid-drop parametrization based on the saturation of the nuclear interaction. The linear dependence at a low H/A is in agreement with theoretical predictions [3] for hypermatter.

The breakup channels are generated according to their statistical weight. In the grand canonics this leads to the following average yields of individual fragments:

$$Y_{AZH} = g_{AZH} \cdot V_f \frac{A^{3/2}}{\lambda_T^3} \exp \left[-\frac{1}{T} (F_{AZH} - \mu_{AZH}) \right], \quad (6)$$

$$\mu_{AZH} = A\mu + Z\nu + H\xi,$$

Here g_{AZH} is the ground-state degeneracy factor of species (A, Z, H) , $\lambda_T = (2\pi\hbar^2/m_N T)^{1/2}$ is the nucleon thermal wavelength, and m_N is the average nucleon mass. The chemical potentials μ , ν , and ξ are responsible for the mass (baryon) number, charge, and strangeness conservation in the system. They can be found from the balance equations:

$$\sum_{AZH} AY_{AZH} = A_0, \quad \sum_{AZH} ZY_{AZH} = Z_0, \quad \sum_{AZH} HY_{AZH} = H_0.$$

Previously we have demonstrated within this model [11] that the fragment mass distributions are quite different for fragments with different strangeness contents. This means that the multifragmentation of excited hypernuclear systems proceeds in a different way compared with conventional nuclei. The reason is the additional binding energy of hyperons in nuclear matter. It was also shown that the yields of fragments with two Λ 's depend

essentially on the binding energy formulas (i.e., on details of ΛN and $\Lambda\Lambda$ interactions) used for the calculations [11, 25]. Therefore, an analysis of double hypernuclei can help to improve these mass formulas and reveal information about the hyperon-hyperon interaction. In Ref. [26] the decay of light excited hypersystems was considered within the framework of the Fermi breakup model. It was also concluded that the production rate of single and double hypernuclei is directly related to their binding energy. In this work we extend our analysis to systems containing up to four hyperons, which may be produced during the dynamical stage of relativistic heavy-ion collisions [16, 23].

III. NEUTRON AND PROTON DRIP LINES OF NORMAL NUCLEI AND HYPERNUCLEI

A. Hypernucleus binding

The treatment of hyperfragments in the freeze-out volume is important in the SMM. As discussed, we have suggested an approach motivated by the successful application of the liquid-drop approximation describing multifragmentation of normal nuclei [7–10]. On the other hand, this approximation suits well for practical using in the developed model. We should note that the properties of the primary fragments may change in the medium compared to the vacuum owing to the proximity of other fragments (see, for example, Ref. [27]). Presently, there is evidence that the symmetry energy [10, 28–30] and surface energy [31] of hot fragments in multifragmentation may be modified. Because the binding energies of hypernuclei are mostly not known even in vacuum, this problem is naturally included in searching for a reliable mass formula for hypernuclei within this approach.

However, it is important to demonstrate the qualitative consistence of the approach at temperature $T = 0$ with the known experimental data and with more sophisticated calculations. Presently, only a few tens of masses of single hypernuclei (mostly light ones) have been experimentally established [1, 24], and only very limited information on double hypernuclei is available. In Fig. 1 we show the experimental data on the separation energy of Λ hyperons in hypernuclei, together with our liquid-drop approximation [Eq. (1)] and with results of relativistic mean-field (RMF) calculations in Refs. [2] and [32].

We see a reasonable agreement and reproduction of the main trend: increasing and

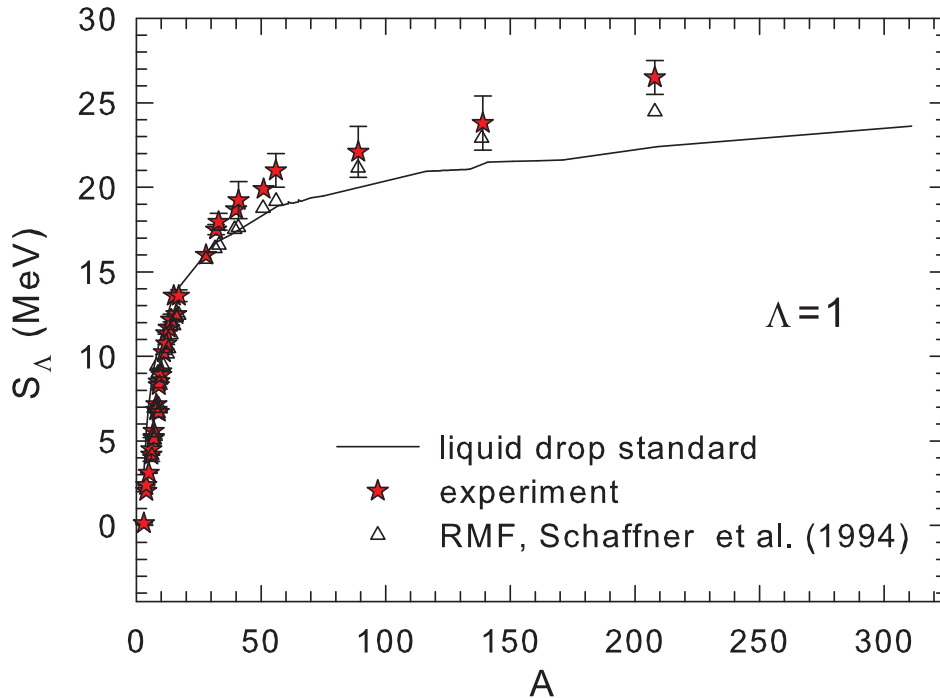


FIG. 1: (Color online) Separation energy of Λ hyperons in hypernuclei versus mass number. The solid line is our liquid-drop approximation at $T = 0$. Stars are experimental data taken from Refs. [1] and [24]. Triangles are results of RMF calculations [2, 32].

saturation of separation energy of hyperons (i.e., their binding energy) with mass number of nuclei. Therefore, the liquid-drop approximation can be used for estimation of single hypernuclei. In Fig. 2 we compare the predictions of the RMF model with our approach for some multiple hypernuclei. There is a similar agreement in binding energies and reproduction of the trend of increasing binding energy with increasing hyperon number.

Moreover, from Figs. 1 and 2 we see that for intermediate-mass and heavy nuclei the predictions of the liquid-drop approximation slightly underestimate hyperon binding, by comparison with both data and RMF. In this case one can say that this approximation provides a low limit for the binding energy in both single and multiple hypernuclei. Note that we consider a number of Λ 's that is much smaller than the total number of baryons. It is sufficient for our purpose to determine the reaction processes leading to formation of exotic and multiple hypernuclei. If the baryonic fraction of hyperons in such nuclei is more than 10–20% , a saturation effect in the binding energy for Λ hypernuclei may take place and they may be converted into Σ and other hyperons [2]. However, a very high strangeness

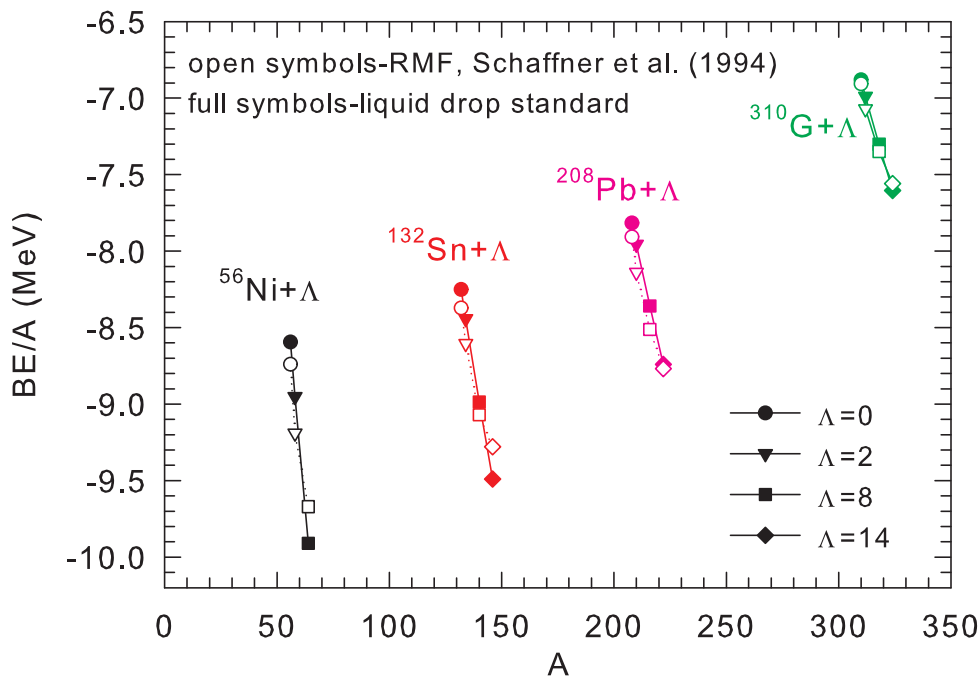


FIG. 2: (Color online) Binding energies (per baryon) of Ni, Sn, Pb, and G ($Z=126$) Λ hypernuclei depending on the number of Λ hyperons. Open symbols are RMF calculations from Refs. [2] and [32], filled symbols, the liquid-drop approximation. Numbers of hyperons considered are shown.

content is beyond the scope of this work.

B. Separation energies of neutrons and protons around drip lines

Neutron and proton drip lines are important for investigating the structure of nuclei. They also play a major role in nucleosynthesis of elements in space. Before moving to hypernuclei it is instructive to recall the behavior of the binding energy in the vicinity of drip lines in normal nuclei. Traditionally, this behavior is evaluated from the separation energies of neutrons and protons. For our purpose it is more convenient to use the separation energies of two neutrons and two protons, in order to avoid the well-known pairing correlations:

$$S_{2n} = BE(A, Z) - BE(A - 2, Z), \quad S_{2p} = BE(A, Z) - BE(A - 2, Z - 2), \quad (7)$$

where $BE(A, Z)$ is the nucleus binding energy.

In Fig. 3 we show the two-neutron separation energies for fluorine ($Z=9$), molybdenum ($Z=42$), and lead ($Z=82$) over a wide range of neutron numbers. We have plotted the

available experimental data taken from [33] together with some sophisticated calculations: RMF [34], the finite-range liquid-drop model (FRDM) [35], the infinite nuclear matter model (INM) [36], a model with Skyrme forces (SkM) [37], the Wigner-Kirkwood mean-field approximation (WK) [38], the standard averaging method in the mean-field approximation (SAM) [38], and Skyrme Hartree-Fock (SKF) [39]. These models were specially constructed to describe nuclear structure and, unfortunately, cannot be directly used in a model of nuclear reactions. We have also shown the results of our liquid-drop approximation, obtained from Eq. (1), at $T = 0$. One can see that it is sufficient for qualitative description of the data and the main trends. The discrepancies come from the shell structure of cold isolated nuclei. On the other hand, in multifragmentation reactions we expect to deal with hot nuclei in the surroundings of other nuclear species. As reported previously these structure effects should be washed out at high temperatures ($T > 1 - 2$ MeV) [40, 41]. It is interesting that some calculations (e.g., the RMF in Ref. [34] for Mo) predict structure effects, like islands of stability, at large numbers of neutrons N .

We have investigated how modifications of the liquid-drop parameters may change our results. In all panels in Fig. 3 we demonstrate effects of a modification of the symmetry term [Eq. (4)], which is crucially important for these separation energies. Instead of the standard parametrization $F^{\text{sym}} = \gamma(A - 2Z)^2/A$, we have divided it into the volume and surface symmetry energy contributions, as suggested in some works [42]. Our aim is to compare the obtained trends, therefore, we have normalized the parametrizations at ^{21}F , ^{102}Mo , and ^{209}Pb , respectively. As a result we found that the symmetry energy coefficient γ increases with mass number; for example, for molybdenum $F_m^{\text{sym}} = (34 - 42/A^{1/3})(A - 2Z)^2/A$. One can see from Fig. 3 that for all elements this division may slightly improve the description of small nuclei, however, it makes the description worse for large nuclei in the vicinity of the drip line. We conclude that inclusion of the surface symmetry energy into consideration does not help to explain the observed behavior of the neutron separation energy around the neutron drip line. On the other hand, if we simply decrease the γ coefficient in Eq. (4) from 25 to 14 MeV we obtain a trend that is less steep with N and that is more consistent with the experimental trend for neutron-rich isotopes. It is interesting that this kind of decrease in symmetry energy was obtained in recent analyses of experimental data on multifragmentation [10, 29, 30]. In this respect, one may speculate that the halo neutrons of such exotic nuclei interact with the core nucleons in a universal way, which looks

like interactions between nuclear species taking place at dilute densities of the freeze-out in multifragmentation reactions.

By analogy, in Fig. 4 we show the two-proton separation energy for isotones with numbers of neutrons equal to 8, 28, and 82. One can see the qualitative consistence of our approximation with experimental data and various nuclear structure calculations. By examining the influence of modifications of the symmetry energy on this separation energy, the parametrizations were normalized at $Z=9$, 24, and 60, respectively. The obtained trends for all masses are similar to those presented in Fig. 3. Therefore, the main conclusions drawn from analysis of Fig. 3 are valid for this case too.

C. Influence of hyperons on separation energies in nuclei

The presence of hyperons inside nuclei increases their binding energies, because of hyperons coupling with nucleons; see Eq. (5). This influences all structure characteristics of nuclei and is manifested in nuclear fragmentation reactions too [11]. The neutron and proton separation energies will also be higher. We demonstrate these energies versus the number of neutrons and protons in nuclei in Figs. 5 and 6. Calculations were performed as previously with the liquid-drop approximation [Eq. (1)] at $T=0$, for nuclei with different numbers of hyperons.

Examining the neutron drip line region around $S_{2n} = 0$, in Fig. 5, we see that by adding only one Λ hyperon into a Mo nucleus we shift its drip line to the right side by nearly 30 mass units. Very neutron-rich hypernuclei are possible and their weak decay time scale is long compared to the typical strong decay times. This effect is present in both small and heavy nuclei, however, in heavy ones it is more pronounced. Double and multiple hypernuclei are even more bound, therefore, their drip lines are shifted far more to the neutron-rich side. Such a high neutron richness can hardly be obtained in any reaction involving normal nuclei. In this respect, the production of hypernuclei may provide a natural way for accumulation of neutrons in nuclei, which can be realized in special processes.

Analysis of the proton separation energies (Fig. 6) leads to similar conclusions: With an increasing number of hyperons the proton drip lines shift considerably to the side of proton richness. Because of Coulomb interaction this shift is less pronounced than in the neutron case. However, it is still a prominent effect, which could be important for nuclear structure

studies and synthesis of new elements.

We expect that the uncertainties in the hyperon-nucleon binding and the symmetry energy discussed in previous subsections will have only a minor influence on the results, and they will not change our predictions qualitatively. The reason is that the hyperon-nucleon interaction is a well-established fundamental concept in both theory and experiment. Recent experimental observations of very neutron-rich hypernuclei, e.g., the ${}^6_{\Lambda}\text{H}$ hypernucleus [43], are consistent with the predicted trend.

IV. PRODUCTION OF HYPERNUCLEI IN FRAGMENTATION AND MULTIFRAGMENTATION PROCESSES

We analyze the problem of how these neutron-rich and proton-rich hypernuclei can be produced in relativistic ion collisions. It has been investigated for normal nuclei during the last 10–20 years (see, e.g., review [44]). Presently there are extensive experimental projects aimed at this study, for example, the Fragment Separator (FRS) at GSI-Darmstadt, and one is planned for the future FAIR facility too [45].

The main physics idea is the following: Relativistic projectile ions undergo fragmentation/multifragmentation, spallation, and fission processes in interactions with targets. These processes lead to the production of a broad variety of exotic residues that already can be close to the neutron (proton) drip lines. Some of these nuclei can live long enough, in particular, because of their large γ factors. We suggest the use of these relativistic exotic nuclei for new interactions with targets for producing hypernuclei. Mechanisms of such interactions were investigated within transport models [16]. After the dynamical stage of the reaction excited hyperspectator residues are produced, which have practically the same average ratio of neutrons to protons as in projectiles. However, great fluctuation of their masses and isospin content is possible. The final hypernuclei will be produced after disintegration of these excited systems. They will have wide distributions and the hyperon contribution to binding such nuclei will make it possible to obtain many nuclei beyond the traditional drip lines.

Below, this mechanism is illustrated with SMM calculations. As input for the calculations we assume dynamically produced hyperspectators with various masses, isospin contents, temperatures and numbers of absorbed hyperons. As demonstrated in Ref. [16], at a

beam energy of about 20 A GeV, heavy spectators can absorb up to three Λ hyperons with a sizable probability, and absorption of larger numbers of hyperons is feasible. We consider masses of hypernuclei systems that can be naturally produced after the dynamical stage ($A_0 = 50, 100, \text{ and } 200$) and with different isospins. Some calculations at small numbers of absorbed hyperons (up to $H_0 = 2$) were reported in Ref. [11]. Here, in order to generalize the results for hypermatter, in Figs. 7 and 8 we demonstrate results of disintegration calculations for systems with four absorbed hyperons. The temperature range ($T = 3 - 5$ MeV) was adopted in order to investigate the region of coexistence of big and small fragments, typical for liquid-gas-type phase transition in finite systems, which is also observed in multifragmentation reactions [7]. We would like to give examples of systems close to the neutron drip line: For this reason, besides systems with an isospin content of typical large, stable nuclei ($Z_0/A_0 = 0.4$; Fig. 7), we present neutron-enriched systems that, as we conclude after examining Ref. [44], may be obtained after reactions with beams separated by the FRS at FAIR ($Z_0/A_0 = 0.35$; Fig. 8).

One can see a general evolution of the mass distributions with temperature: At a low temperature ($T = 3$ MeV) we have a "U-shape" distribution that consists of two maxima, at the lightest (nucleons and light clusters) and largest (close to the system size) fragments, and the "valley" in between. The yield of intermediate-mass fragments increases with increasing temperature and at about $T = 5$ MeV we obtain a "plateau"-like distribution. At higher temperatures we will have an exponential decrease in yield with mass number [11]. This picture was solidly established in multifragmentation reactions with normal nuclei [7, 9, 10]. However, the presence of hyperons causes interesting consequences: At moderate temperatures hyperons are predominantly accumulated in big fragments because of the high binding energy. At low temperatures, when the largest nuclei survive, one can be sure that they contain practically all the Λ 's of the system. This main result will not change if one considers a canonical statistical ensemble for description of the system's disintegration (see Ref. [12]), though some minor details will be different from the adopted grand canonicity of Eq. (6).

In all the figures one can see a very interesting feature: Curves of fragment yields with different numbers of Λ 's intersect at one point, at a particular A , which is determined by the parameters of the systems. Actually, this has a trivial explanation following the grand canonical structure of Eq. (6) and taking into account Eq. (5): For fragments with any hyperon content there is the same A at which the sum contribution of H into Y_{AZH} becomes

0. This happens when $(10.68 - 21.27/A^{1/3}) + \xi = 0$. As shown in Ref. [11], at very high temperatures ξ becomes too low, the system disintegrates into small pieces only, and the mass distributions of all fragments decrease exponentially with A , without intersection.

An important question for the examination of drip lines is the isotope composition of the produced fragments. For this purpose in Fig. 9 we present the isotope distributions of fluorine and molybdenum elements formed after disintegration of the systems with $A_0 = 200$ at the temperature $T = 4$ MeV and with total charges $Z_0 = 80, 70$, and 60 . Here we attempt to approach the neutron drip line by taking an excess of neutrons over protons. The first two cases give relatively moderate and large isospins in the system, which should be reachable with the FRS in future FAIR experiments. The last system is very neutron rich, however, this high isospin content may be considered as a limit that should be investigated to estimate the usefulness of the suggested method. Actually, in the case of relativistic projectiles, it is sufficient that such nuclear systems coming after the FRS would be rather short-lived (microseconds) in order to use them and generate new reactions leading to production of hypernuclei. As before we assumed that up to four Λ hyperons were initially captured in the systems during the dynamical stage.

One can see in Fig. 9 that the absolute yields of isotopes change with the number of hyperons in fragments. This is related to the difference in mass yields discussed above. On the other hand, the isotope distribution widths look similar. The position of the peak is mainly determined by the system's isospin, however, the widths are quite large. For clarity, in the figure we show isotopes containing even numbers of hyperons only. The yields of isotopes with odd numbers of hyperons are in between the corresponding even numbers.

We have also performed SMM calculations for systems with a smaller number of dynamically captured hyperons ($H_0 = 2$), which are more likely to be obtained in reactions. We have taken into account that the symmetry energy coefficient γ in disintegration reactions may decrease from 25 to 14 MeV as discussed literature [10]. In Fig. 10 we demonstrate a comparison between these calculations for the cases of two neutron-rich systems with large isospins $(A_0, Z_0) = (200, 70)$ and $(200, 60)$. In addition, we show calculations for a proton-rich system with $A_0 = 125$ and $Z_0 = 60$, which is used to estimate possibilities of producing nuclei beyond the proton drip line.

It is known from normal nuclear multifragmentation that a decreasing symmetry energy leads to increasing yields of neutron-rich nuclei [10]. In Fig. 10 we see that the distribution

widths increase considerably at $\gamma = 14$ MeV, and more neutron-rich isotopes can be produced, especially for large elements. For example, the expected neutron drip line for Mo with $N \approx 86 - 88$ can be reached and overpassed already after disintegration of a system with a moderately large isospin ($Z_0 = 70$). If it is possible to get secondary beams with even larger isospins, then, certainly, there will be abundant production of nuclei beyond the drip line. There is the same effect for fluorine too. Moreover, as shown in Fig. 10 the isotope distributions of normal nuclei (noted by $\Lambda=0$) behave similarly to those of hypernuclei. This can be explained simply by the same structure of the symmetry energy; see Eq. (4). In this respect, using isospin-enriched relativistic beams for secondary interactions is a very promising method for study of normal nuclei too. However, a big advantage of hyperfragments is that they are more stable, as the separation energies of nucleons are essentially higher. Therefore, neutrons that are accumulated in nuclei in the freeze-out volume will not leave them during the time scale of strong interaction when these nuclei leave the freeze-out. Possible secondary de-excitation processes will also affect these nuclei less, because of the high binding energy.

Generally, the reaction mechanisms used in our approach suggest that proton-rich nuclei and proton-rich hypernuclei can be obtained in similar ways. This is a consequence of the regular behavior of neutron and proton separation energies (see Figs. 5 and 6). We have checked it by calculating just proton-rich systems. The general evolution of mass yields of fragments and hyperfragments with temperature is the same as shown in Figs. 7 and 8. The main conclusions regarding isotope production are also the same, as one can see in the bottom panels in Fig. 10. One can get proton-rich hyperfragments beyond the proton drip lines, which could also be stable with respect to strong decay.

In the following these exotic proton- and neutron-rich Λ hypernuclei will decay in weak processes. For heavy nuclei we expect predominantly nonmesonic decay producing two fast nucleons, like $\Lambda N \rightarrow NN$. With a considerable probability these nucleons can leave the nucleus without interactions, therefore, the large neutron/proton content of the nucleus will be preserved. This process gives us the opportunity, with the help of hypernuclei, to move beyond the drip lines in normal nuclei too and investigate islands of stability that may exist (e.g., [3] and [34]). This is a new method for obtaining such proton- and neutron-rich nuclei. The involvement of hyperons may provide a unique reaction mechanism to obtain nuclei with exotic isospins and to study both the proton and the neutron sides of the nuclear chart.

V. CONCLUSION

New promising reaction mechanisms for production of hypernuclei are under theoretical investigation. The dynamical stage of relativistic ion collisions can lead to the production of hyperons, which are captured by spectator residues. Disintegration of these hot residues leads to production of hypernuclei. This process was previously associated with the liquid-gas-type phase transition in finite nuclear systems and it provides the opportunity to study hypernuclear matter at subnuclear densities too. We demonstrate a broad variety of hypernuclei obtained in this way. The generalized SMM applied previously for description of disintegration processes in normal nuclei is also a good candidate to describe the hypernuclear case. We show that the nucleon separation energies in hypernuclei become considerably higher than in normal nuclei, because of coupling hyperons and nucleons inside nuclei. This makes it possible to obtain very exotic hypernuclei in these reactions, which can go far beyond the drip lines established for normal nuclei. Investigation of such hypernuclei will help to answer many fundamental questions of hyperphysics and nuclear physics. Moreover, the production of exotic hypernuclei in these reactions followed by their weak decay is a novel process which can be used to obtain normal exotic nuclei beyond the drip lines. It may provide a unique chance to investigate nuclear islands of stability. Presently, there are quite limited possibilities of obtaining such exotic hypernuclei with other experimental methods. We believe that hypernuclear and nuclear physics will benefit strongly from the exploration of new production mechanisms for hypernuclei associated with spectator fragmentation reactions.

Acknowledgments

This work was supported by the the GSI Helmholtzzentrum für Schwerionenforschung and Hessian initiative for excellence (LOEWE) through the Helmholtz International Center for FAIR (HIC for FAIR), and by the Helmholtz-Institut Mainz. N.B. and A.S.B. thank the Frankfurt Institute for Advanced Studies and the Institut für Kernphysik of J.Gutenberg-Universität Mainz for hospitality. We also acknowledge the support from the Research Infrastructure Integrating Activity Study of Strongly Interacting Matter HadronPhysics3

under the Seventh Framework Programme of the EU (SPHERE network).

- [1] O. Hashimoto and H. Tamura, *Prog. Part. Nucl. Phys.* **57**, 564 (2006).
- [2] J. Schaffner, C.B. Dover, A. Gal, C. Greiner, and H. Stoecker, *Phys. Rev. Lett.* **71**, 1328 (1993).
- [3] W. Greiner, *J. Mod. Phys. E* **5**, 1 (1995).
- [4] P. Papazoglou, S. Schramm, J. Schaffner-Bielich, H. Stoecker, and W. Greiner, *Phys. Rev. C* **57**, 2576 (1998)
- [5] J. Schaffner-Bielich, *Nucl. Phys. A* **804**, 309 (2008).
- [6] M. Danysz and J. Pniewski, *Philos. Mag.* **44**, 348 (1953).
- [7] J. P. Bondorf, A. S. Botvina, A. S. Iljinov, I. N. Mishustin, and K. Sneppen, *Phys. Rep.* **257**, 133 (1995).
- [8] H. Xi et al., *Z. Phys. A* **359**, 397 (1997).
- [9] R. P. Scharenberg et al., *Phys. Rev. C* **64**, 054602 (2001).
- [10] R. Ogul *et al.*, *Phys. Rev. C* **83**, 024608 (2011).
- [11] A. S. Botvina and J. Pochodzalla, *Phys. Rev. C* **76**, 024909 (2007).
- [12] S. Das Gupta, *Nucl. Phys. A* **822**, 41 (2009); V. Topor Pop and S. Das Gupta, *Phys. Rev. C* **81**, 054911 (2010).
- [13] M. Wakai, H. Bando, and M. Sano, *Phys. Rev. C* **38**, 748 (1988).
- [14] Z. Rudy and W. Cassing *et al.*, *Z. Phys. A* **351**, 217 (1995).
- [15] Th. Gaitanos, H. Lenske, and U. Mosel, *Phys. Lett. B* **675**, 297 (2009).
- [16] A. S. Botvina, K. K. Gudima, J. Steinheimer, M. Bleicher, I. N. Mishustin, *Phys. Rev. C* **84**, 064904 (2011).
- [17] J. Steinheimer, K. Gudima, A. Botvina, I. Mishustin, M. Bleicher, and H. Stoecker. *Phys. Lett. B* **714**, 85 (2012).
- [18] K. J. Nield et al., *Phys. Rev. C* **13**, 1263 (1976).
- [19] S. Avramenko et al., *JETP Lett.* **48**, 516 (1988); S. Avramenko et al., *Nucl. Phys. A* **547**, 95c (1992).
- [20] T. R. Saito *et al.* (HypHI Collaboration), *Nucl. Phys. A* **881**, 218 (2012).
- [21] The STAR Collaboration, *Science* **328**, 58 (2010).

- [22] A. S. Botvina, I. N. Mishustin, and J. Pochodzalla, Phys. Rev. C **86**, 011601(R) (2012).
- [23] A. S. Botvina *et al.*, Nucl. Phys. A **881**, 228 (2012).
- [24] H. Bando, T. Motoba, and J. Zofka, Int. J. Mod. Phys. A **5**, 4021 (1990).
- [25] C. Samanta, P. R. Chowdhury, and D. N. Basu, J. Phys. G: Nucl. Part. Phys. **32**, 363 (2006).
- [26] A. S. Lorente, A. S. Botvina, and J. Pochodzalla, Phys. Lett. B **697**, 222 (2011).
- [27] S. Typel, J. Phys. Conf. Ser. **413**, 012026 (2013).
- [28] A. Le Fèvre *et al.*, Phys. Rev. Lett. **94**, 162701 (2005).
- [29] J. Iglio *et al.*, Phys. Rev. C **74**, 024605 (2006).
- [30] G. A. Souliotis, A. S. Botvina, D. V. Shetty, A. L. Keksis, M. Jandel, M. Veselsky, and S. J. Yennello, Phys. Rev. C **75**, 011601 (2007).
- [31] A. S. Botvina, N. Buyukcizmeci, M. Erdogan, J. Lukasik, I. N. Mishustin, R. Ogul, and W. Trautmann, Phys. Rev. C **74**, 044609 (2006).
- [32] J. Schaffner, C. B. Dover, A. Gal, C. Greiner, D. John Millener, and H. Stöcker, Ann. of Phys. **235**, 35 (1994).
- [33] G. Audi, A. H. Wapstra, and C. Thibault, Nucl. Phys. A **729**, 337 (2003).
- [34] A. H. Yilmaz and T. Bayram, J. Korean Phys. Soc., **59**, 3329 (2011).
- [35] P. Möller, J. R. Nix, and K.-L. Kratz, Atom. Data and Nucl. Data Tables **66**, 131 (1997).
- [36] R. C. Nayak and L. Satpathy, Atom. Data and Nucl. Data Tables **98**, 616 (2012).
- [37] E. Chabanat, R. Bonche, R. Haensel, J. Meyer, R. Schaeffer, Nucl. Phys. A **635** 231 (1998).
- [38] W. Nazarewicz, T. R. Werner, and J. Dobaczewski, Phys. Rev. C **50**, 2860 (1994).
- [39] B. A. Brown, R. R. C. Clement, H. Schatz, A. Volya, and W. A. Richter, Phys. Rev. C **65**, 045802 (2002).
- [40] A. V. Ignatiuk, Phys. Lett. B **76**, 543 (1978).
- [41] M. V. Ricciardi *et al.*, Nucl. Phys. A **733**, 299 (2004).
- [42] W. D. Myers and W. J. Swiatecki, Nucl. Phys. **81**, 1 (1966).
- [43] M. Agnello *et al.*, Nucl. Phys. A **881**, 269 (2012).
- [44] Th. Aumann, Prog. Part. Nucl. Phys. **59**, 3 (2007).
- [45] H. Geissel *et al.*, Nucl. Inst. Meth. Phys. Res. B **204**, 71 (2003).

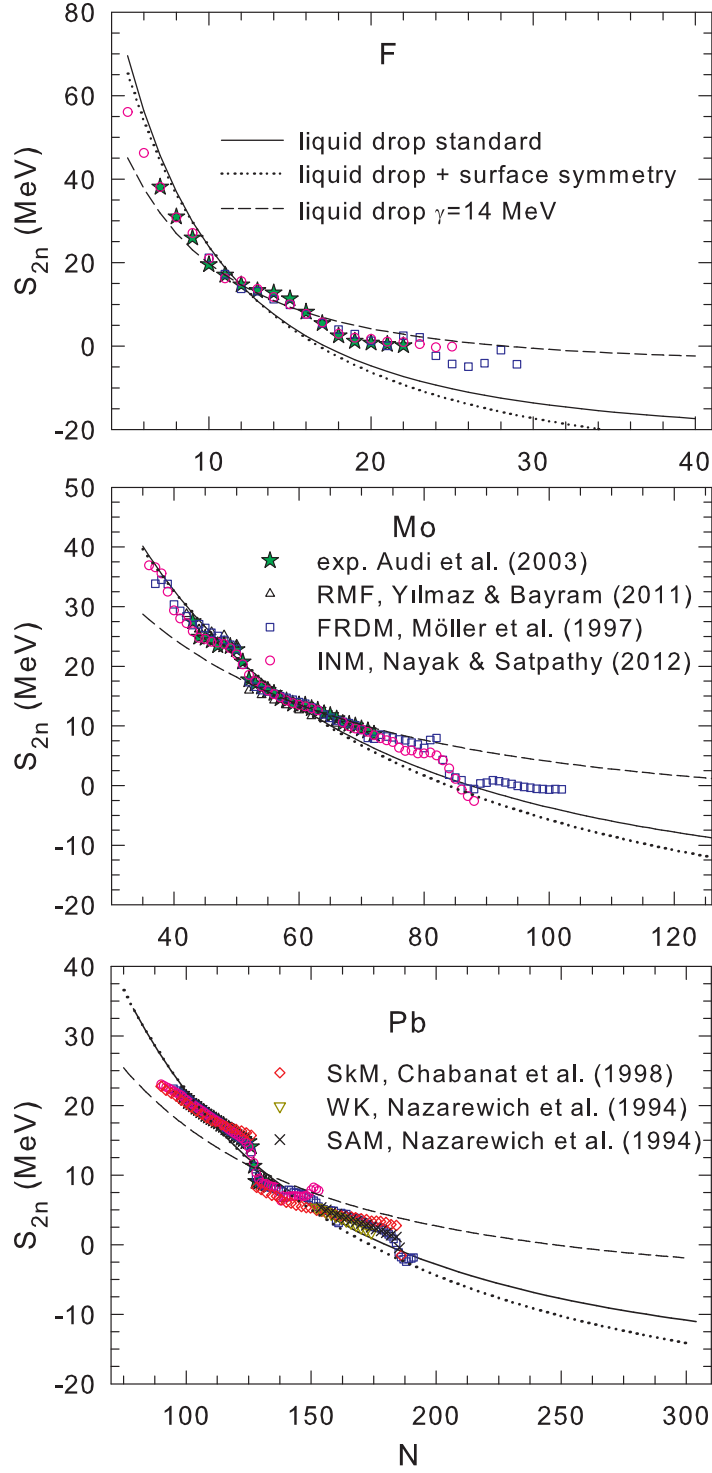


FIG. 3: (Color online) Separation energy of two neutrons in fluorine ($Z=9$), molybdenum ($Z=42$), and lead ($Z=82$) nuclei versus neutron number. Stars are experimental data [33]; symbols are model calculations (see also the text). Lines are the liquid-drop approximation used in the SMM: solid line, standard symmetry energy coefficient ($\gamma = 25$ MeV); dashed line, reduced symmetry energy ($\gamma = 14$ MeV); dotted line, including the surface symmetry energy contribution (see the text).

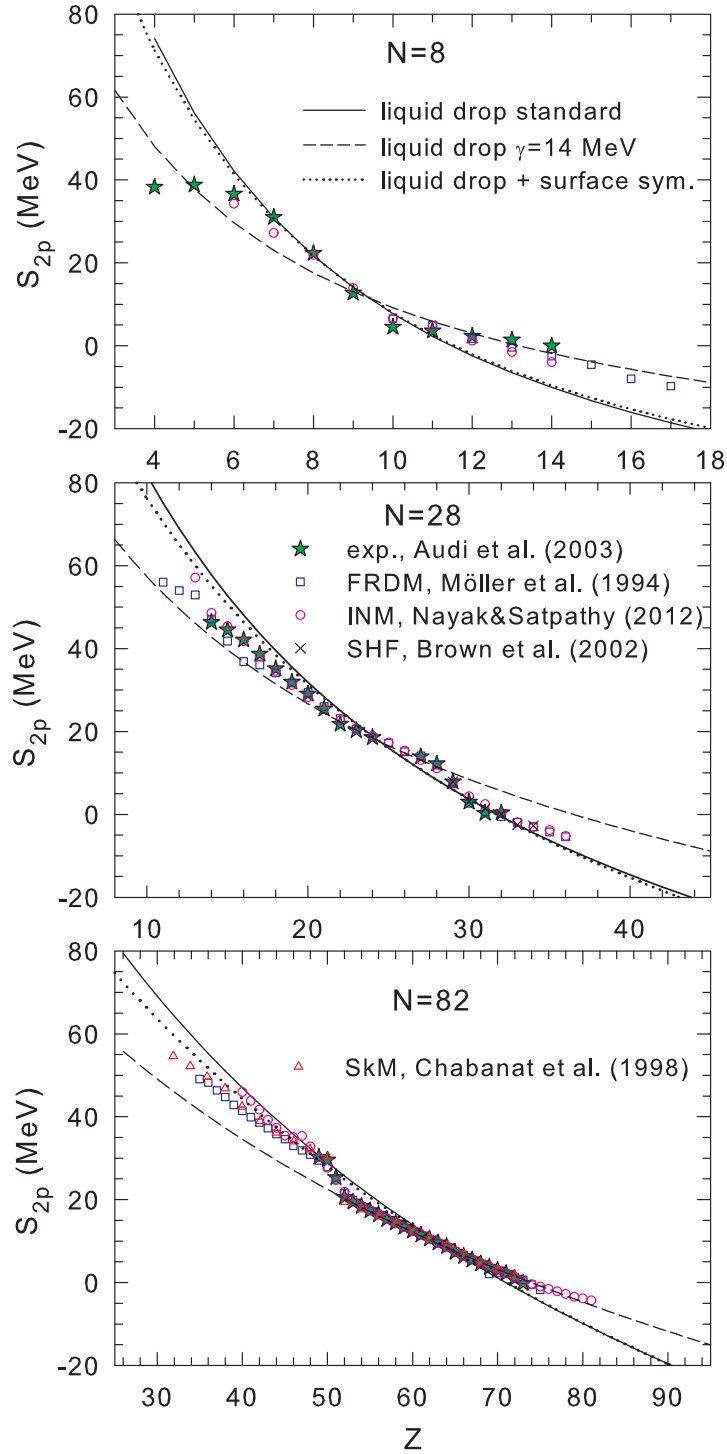


FIG. 4: (Color online) Separation energy of two protons in nuclei containing 8, 28, and 82 neutrons versus proton number. Stars are experimental data [33]; symbols are model calculations (see also the text). Lines are liquid-drop approximations used in the SMM, as in Fig. 3 (see the text).

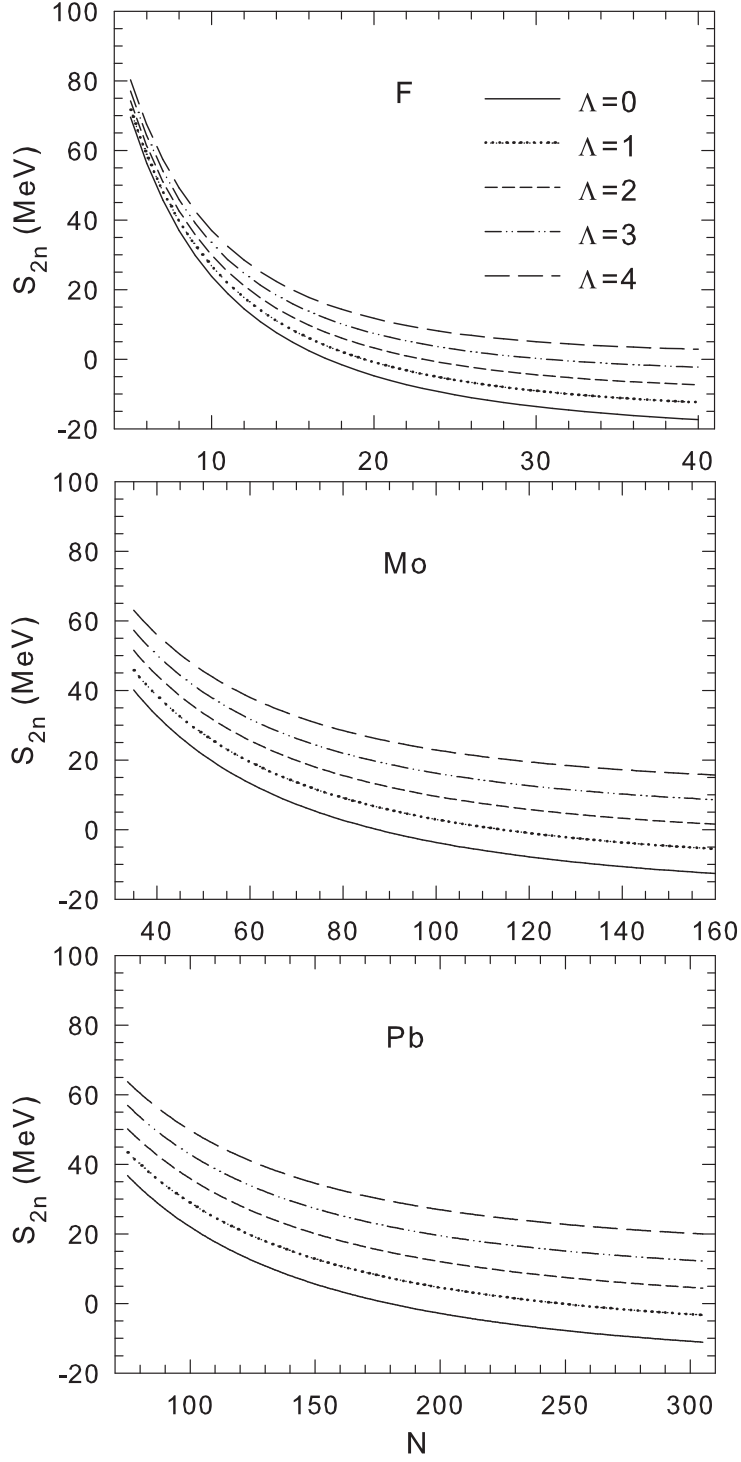


FIG. 5: Separation energy of two neutrons in hypernuclei of fluorine, molybdenum, and lead, versus neutron number. Lines give different numbers of Λ hyperons inside nuclei, according to the liquid-drop approximation (see the text).

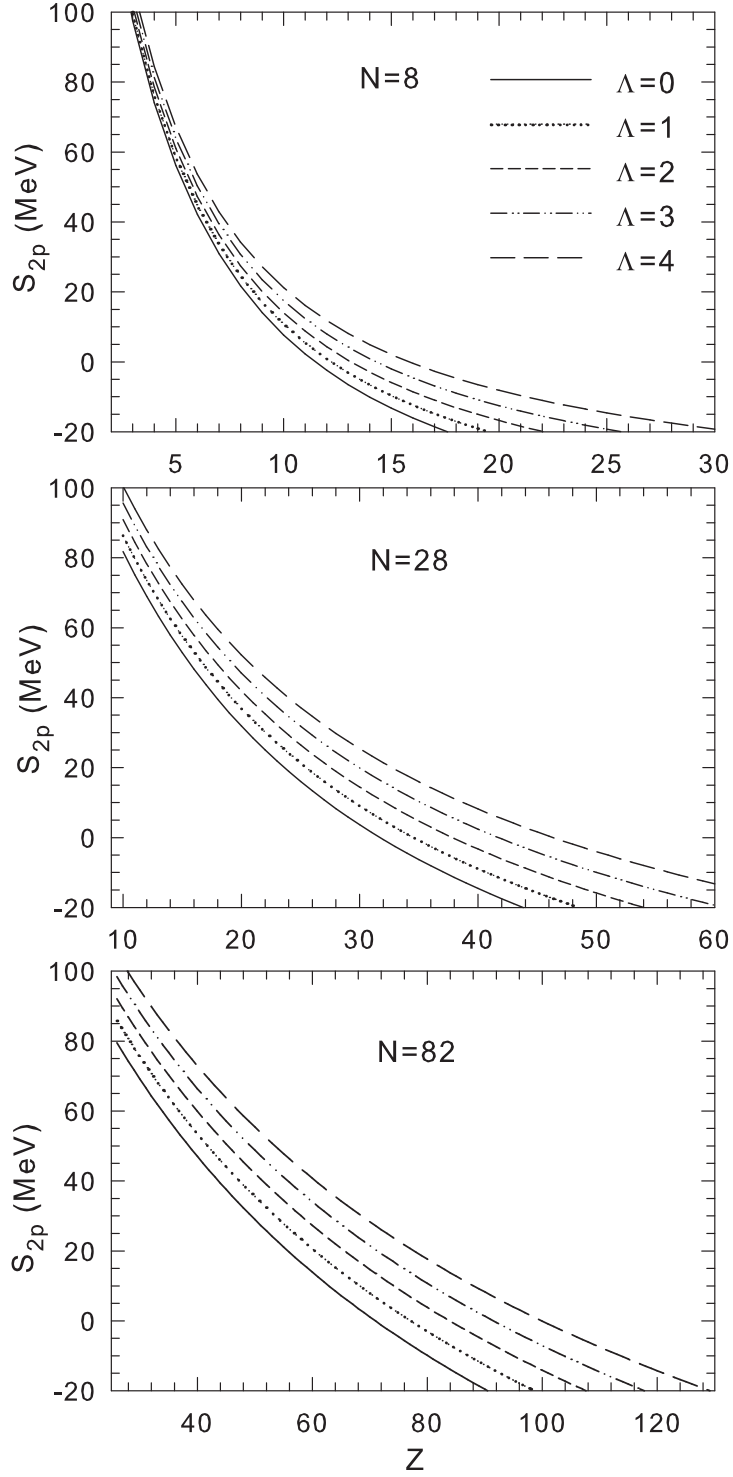


FIG. 6: Separation energy of two protons in hypernuclei containing 8, 28, and 82 neutrons versus proton number. Lines give different numbers of Λ hyperons inside nuclei, according to the liquid-drop approximation (see the text).

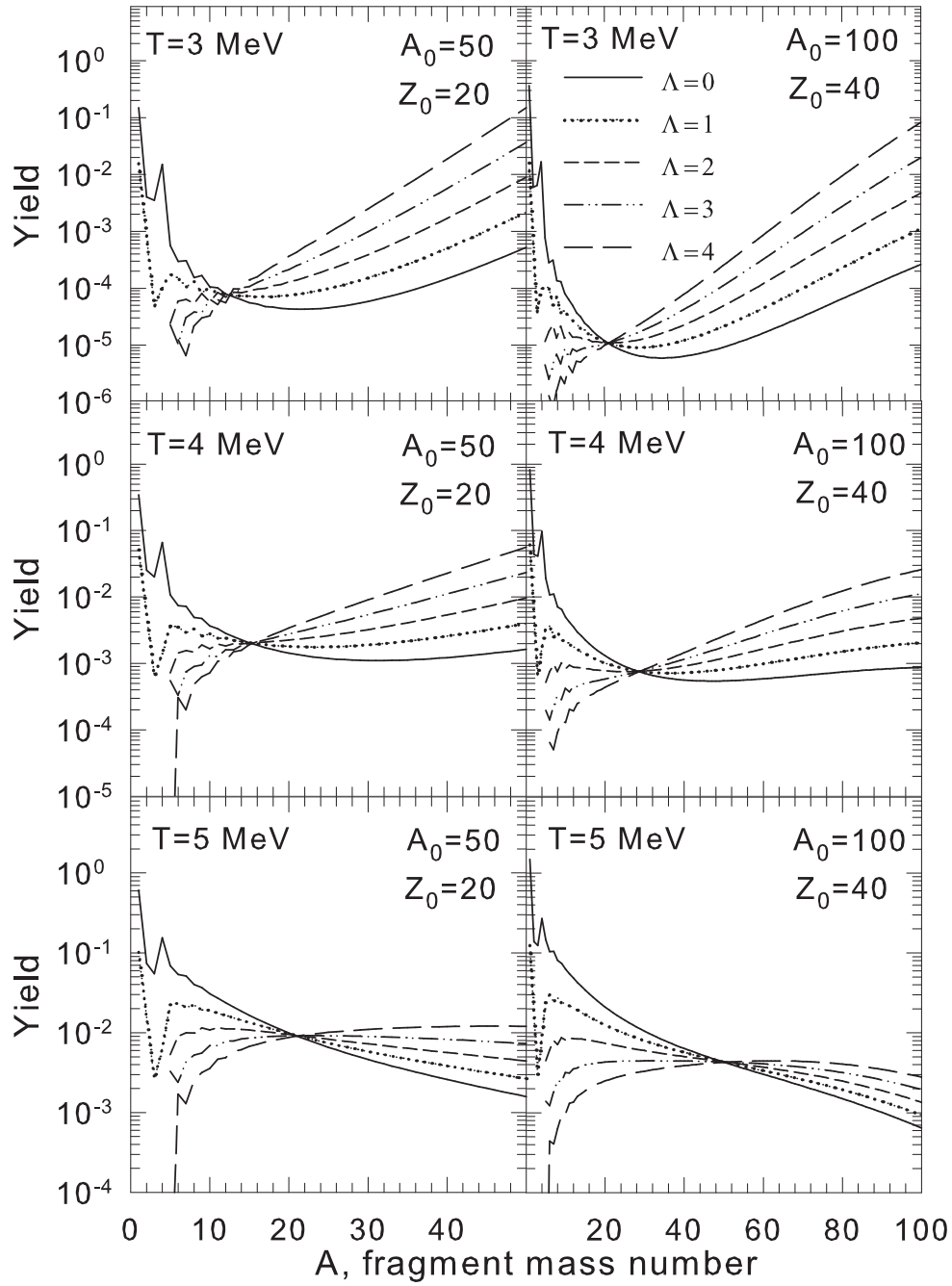


FIG. 7: SMM predictions of yields of fragments and hyperfragments versus their mass number, after disintegration of excited systems containing four Λ hyperons. Initial mass numbers A_0 , charges Z_0 , and temperatures T of the systems are shown. Lines are calculations for fragments with a certain number of Λ hyperons. Yields are given per one disintegration event.

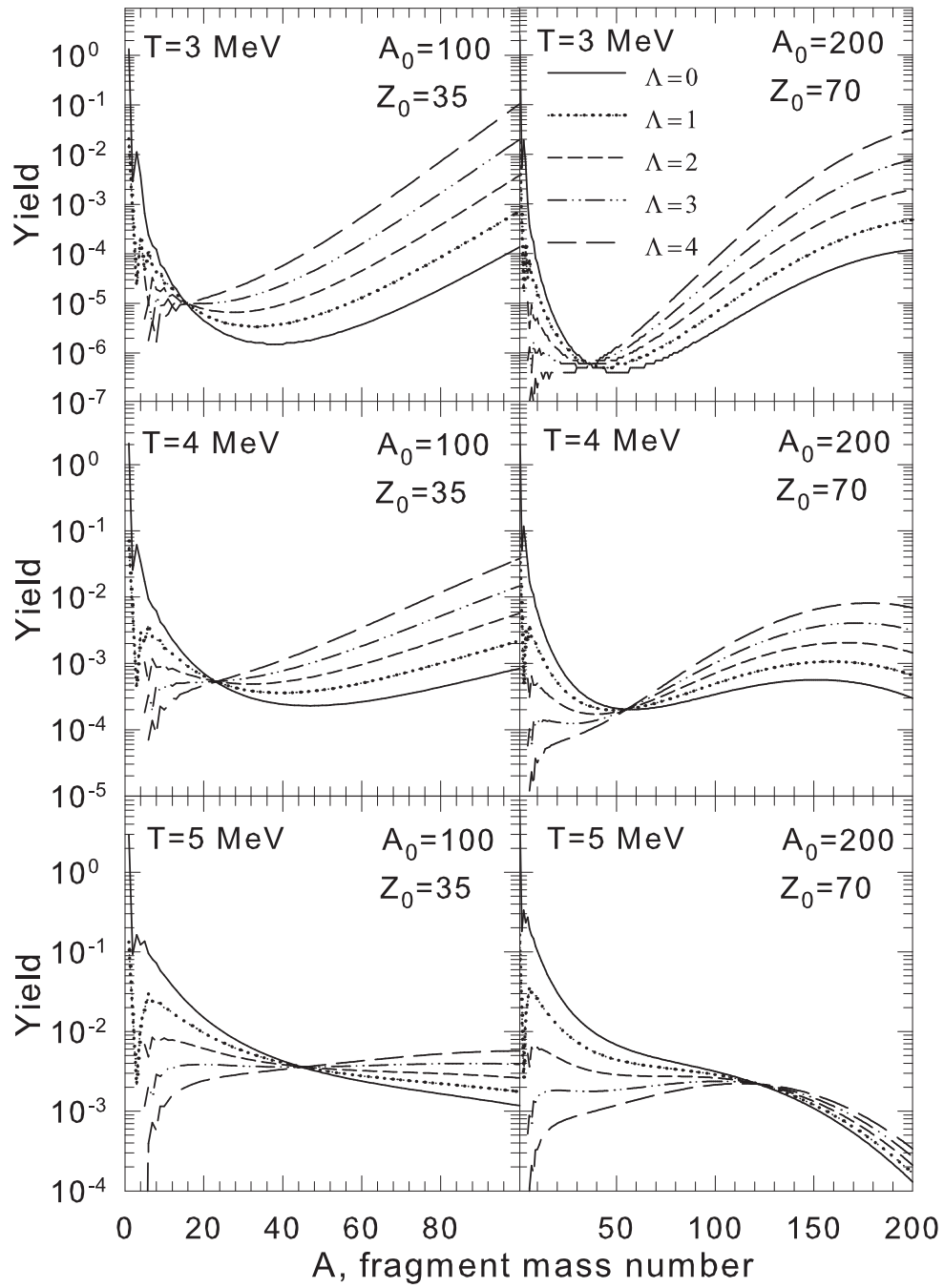


FIG. 8: The same as Fig. 7, but for other neutron-rich systems.

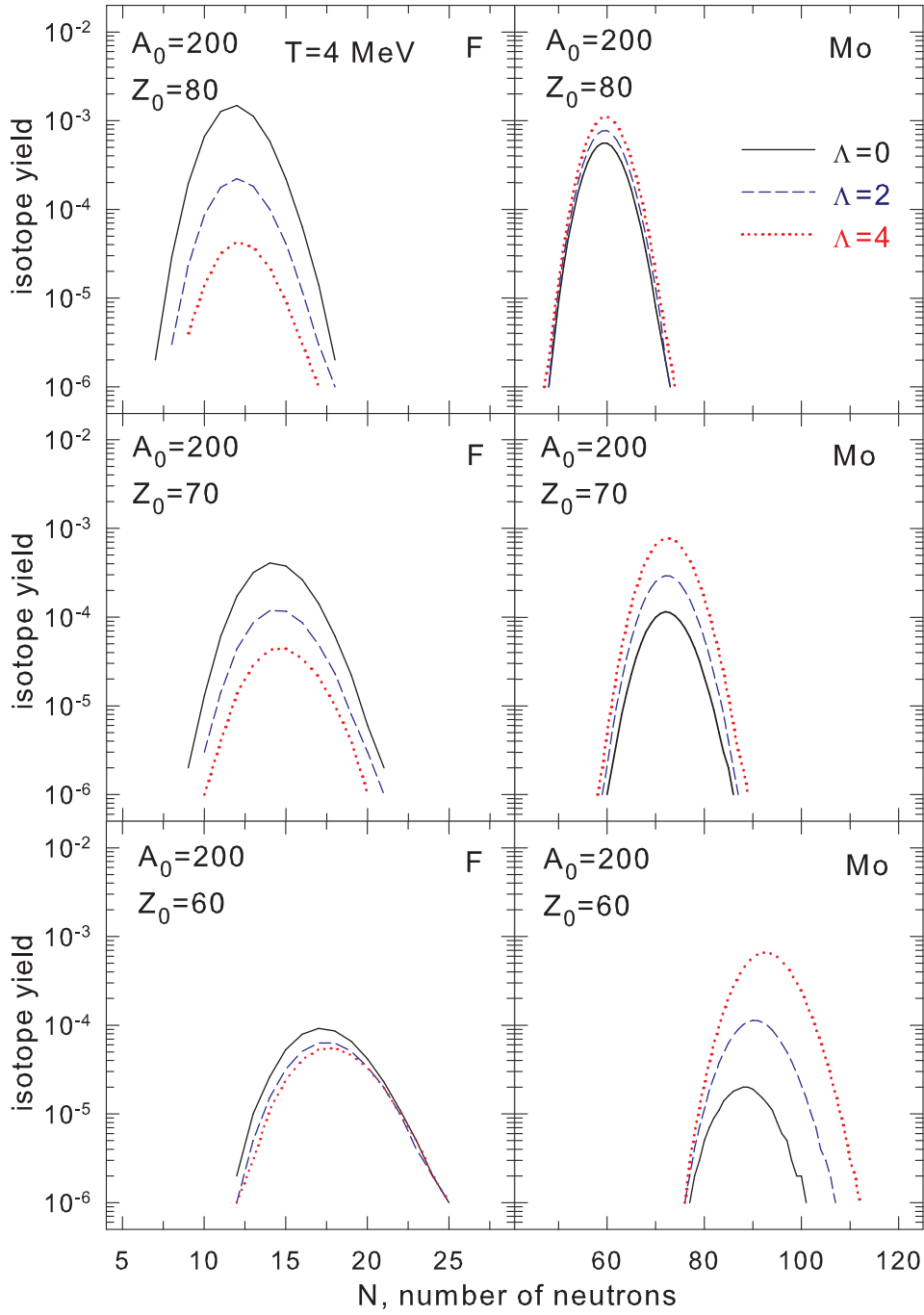


FIG. 9: (Color online) Isotope yields of nuclei and hypernuclei of fluorine (F) and molybdenum (Mo) elements versus their neutron number (N) as calculated by the standard SMM for temperature $T = 4$ MeV and for a system initially containing four Λ hyperons. Initial mass numbers A_0 and charges Z_0 are shown. Lines are calculations for nuclei produced with a certain number of Λ hyperons.

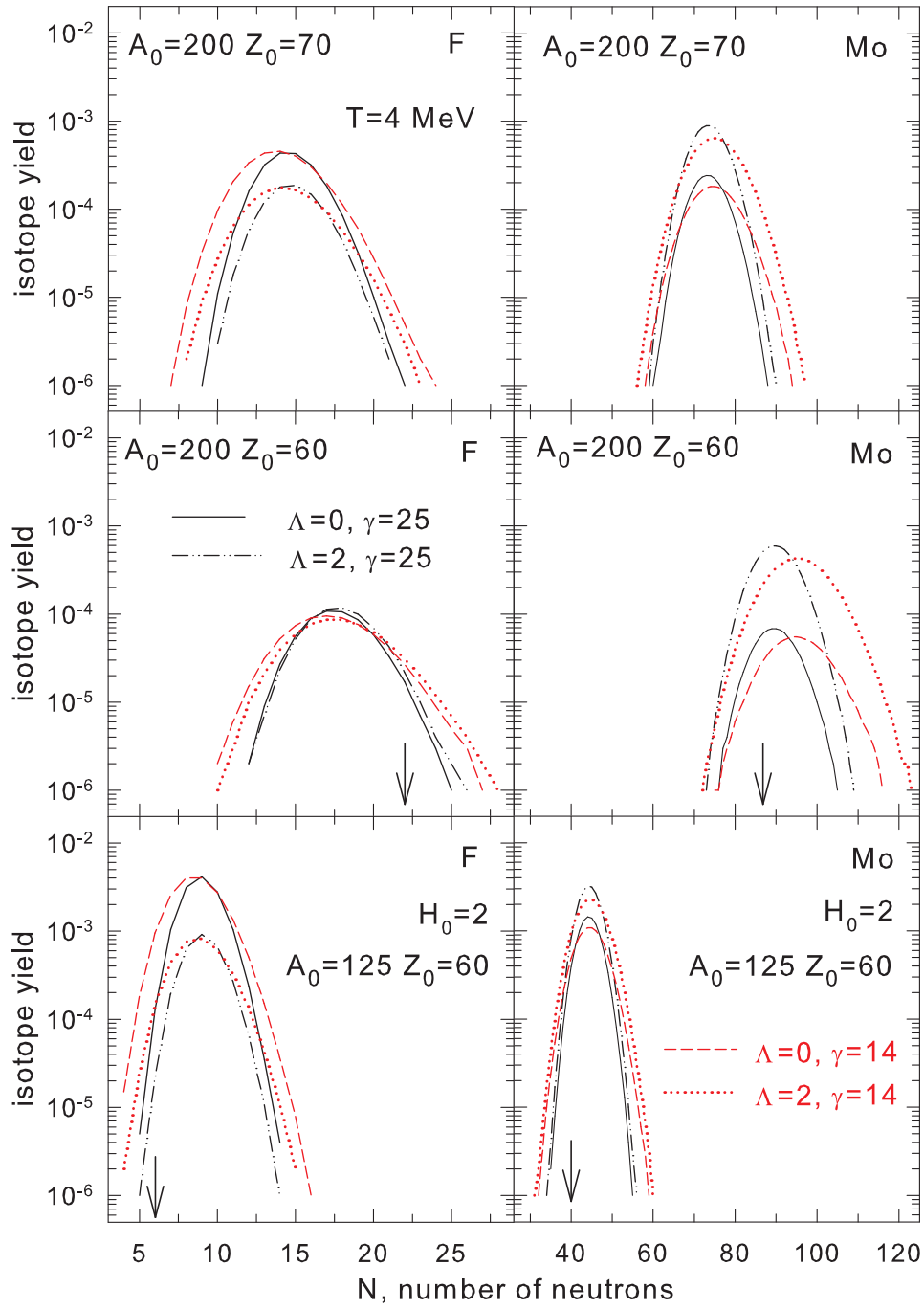


FIG. 10: (Color online) The same as Fig. 9, but for systems initially containing $H_0 = 2$ Λ hyperons. Calculations with the standard symmetry energy coefficient $\gamma = 25$ MeV and the reduced symmetry energy $\gamma = 14$ MeV are presented. Arrows indicate approximate numbers of neutrons corresponding to the neutron and proton drip lines.